SCIENCE CHINA
Chemistry

•ARTICLES•

https://doi.org/10.1007/s11426-024-2460-1

Unveiling phosphofructokinase as the key target: an innovative strategy combining pull-down assays with optical imaging for snail-killing mechanism exploration

Yuxun Lu[1,3†], Weisi Wang[2†], Le Yu[1], Yu-Qiang Zhao[1,5], Ying Chen[2], Yunhai Guo[2], Bing-Rong Luo[4], Yu-Hua Liu[4], Shizhu Li[2*], Liping Duan[2*] & Ying Zhou[1*]

[1]*Yunnan Characteristic Plant Extraction Laboratory, College of Chemical Science and Technology, Yunnan University, Kunming 650500, China*
[2]*National Institute of Parasitic Diseases, Chinese Center for Disease Control and Prevention (Chinese Center for Tropical Diseases Research); NHC Key Laboratory of Parasite and Vector Biology; WHO Collaborating Centre for Tropical Diseases; National Center for International Research on Tropical Diseases, Shanghai 200025, China*
[3]*College of Biological and Chemical Engineering, Guangxi University of Science and Technology, Liuzhou 545005, China*
[4]*Dali Institute of Schistosomiasis Control, Dali 671000, China*
[5]*School of Chemistry and Environment, Yunnan Minzu University, Kunming 650500, China*

Received October 12, 2024; accepted December 5, 2024; published online January 3, 2025

The *Pomacea canaliculata*, also known as apple snail, is an invasive species in China, posing a serious threat to agricultural production and public health. To prevent its rampant infestation, we developed a highly efficient snail-killing lead compound, 1-(4-chlorophenyl)-3-(pyridin-3-yl)urea (PBQ). However, the killing mechanism of PBQ remains unclear. To elucidate this, two novel compounds, **B-PBQ** and **J-PBQ**, were developed through structural modification of PBQ and were used, through both protein pull-down assay and confocal laser scanning microscopy imaging, to identify and confirm that phosphofructokinase (PFK) in the apple snail is the primary target protein of PBQ. Further studies revealed that PBQ successfully inhibits the activity, content, and expression of PFK in apple snail, disrupting the glycolysis pathway and leading to abnormal energy production. These disruptions impair the snail's tolerance to low oxygen, resulting in its efficient eradication. These findings offer a promising direction for developing next-generation PFK-targeted snail-killing pesticides. Furthermore, the strategy of combining pull-down assays with optical imaging used in this work provides a novel approach for the exploration of mechanisms of other pesticide candidates.

molluscicide, phosphofructokinase (PFK), killing mechanism, chemical proteomics, optical imaging

Citation: Lu Y, Wang W, Yu L, Zhao YQ, Chen Y, Guo Y, Luo BR, Liu YH, Li S, Duan L, Zhou Y. Unveiling phosphofructokinase as the key target: an innovative strategy combining pull-down assays with optical imaging for snail-killing mechanism exploration. *Sci China Chem*, 2025, 68, https://doi.org/10.1007/s11426-024-2460-1

1 Introduction

As an invasive species, *Pomacea canaliculata* (*P. canaliculata*) poses a threat to global food security and affects the agricultural ecological environment by reducing the quality of water in which it resides and damaging local freshwater organisms [1,2]. Additionally, *P. canaliculata* is the intermediate host of *Angiostrongylus cantonensis* [3], also known as the rat lung nematode, which is a parasitic nematode causing eosinophilic meningitis in humans [4]. Thus, *P.*

†Equally contributed to this work.
*Corresponding authors (email: lisz@chinacdc.cn; duanlp@nipd.chinacdc.cn; yingzhou@ynu.edu.cn)

canaliculata poses a major threat to environmental safety, agriculture, and human health. Although physical and biological control are worthwhile prevention measures of *P. canaliculata* invasion, chemical control remains the most effective measure [5].

Over recent decades, molluscicides have been commonly used as snail control strategies by governments and public health agencies [6]. To date, the niclosamide is the most widely used chemical and is also the only molluscicide recommended by the WHO [7]. However, niclosamide is highly toxic to non-target aquatic organisms within snail habitats, especially fish, which greatly limits its acceptability in some circumstances [8,9]. Metaldehyde is also a widely used and highly effective molluscicide but it also poses risks of high toxicity to non-target organisms [10]. Alternative molluscicides that are safer and more specific would be beneficial in the fight against snails and their related parasitic diseases.

Our previous studies have identified a novel environmentally friendly molluscicide 1-(4-chlorophenyl)-3-(pyridin-3-yl) urea (PBQ; also known as PPU06) with excellent snail-targeting specificity (Scheme 1A). PBQ exhibited strong molluscicidal potency against *P. canaliculata*, *Oncomelania hupensis*, and *Biomphalaria straminea*, the snail hosts of *A. cantonensis*, *Schistosoma japonicum* and *Schistosoma mansoni* [11–13]. PBQ also showed a good safety profile in mammals and non-target species, including *Danio rerio*, *Daphnia magna*, *Neocaridina denticulata*, *Eriocheir sinensis*, and *Apis mellifera L* [11,14]. Application of PBQ in fields is considered a feasible and environmentally friendly strategy to reduce populations of snail hosts in endemic areas [11,14]. However, despite the above encouraging findings, the molecular mechanism of the lethal molluscicidal action of PBQ has not yet been elucidated.

Using biotin and fluorophore-modifying drugs is an effective means to study drug mechanism of action [15,16]. In 2015, Wang *et al*. [17] used biotin to modify artemisinin derivatives and highlighted 124 artemisinin covalent-binding protein targets. Additionally, using fluorescent dye binding, heme was shown to be responsible for artemisinin activation, providing evidence of the mechanism by which artemisinin kills parasites. Similarly, to investigate the mechanism of action of chloroquine, Gao *et al*. [18] developed a new clickable, photoaffinity chloroquine simulation probe that retains its antimalarial activity. Using this probe, they identified 40 proteins that could be possible antimalarial targets of chloroquine, and found that chloroquine disrupts glycolysis and energy metabolism in malaria parasites by directly binding to a number of key enzymes.

Fluorescence analysis is a simple, fast, and efficient technique that enables the intuitive detection of targets in biological samples by using fluorescent probes [19–28]. Our research group [29] has long worked on the development of fluorescent small-molecule probes and recently reported on a probe termed L4OD, which can detect cytochrome P450 reductase and imaging in tumor cells and mouse tumors. In 2021, we developed a near-infrared fluorescent probe, termed Niap, capable of identifying alkaline phosphatase. Using Niap, we found that PBQ mainly stimulated increased alkaline phosphatase in the liver of the snail and had less influence in the foot and stomach, providing optical evidence of the effect of PBQ on the snail and suggesting that the liver of the snail may be the target of drug action [30].

Herein, we use a combination of chemical proteomics, enzymatic assays, fluorescent probing, and in silico docking approaches to identify target proteins of PBQ and gain insights into molluscicidal mechanism of action in *P. canaliculata* (Scheme 1B). Our data demonstrated that 6-phosphofructokinase (PFK) is the active target of PBQ and predominantly responsible for snail killing (Scheme 1C). In addition, difference in the phylogenetics and protein sequence of PKF homologues confers the high efficacy of PBQ against the snails while the minimum side effects towards nontarget species. Overall, this work elucidates the mechanism and specificity of PBQ in snail killing and has implications for the design and development of novel and better alternative molluscicides against infectious disease snail hosts.

2 Results and discussion

2.1 Successful preparation and activity testing of the two modified molecules

To identify the target proteins of PBQ, two small molecules were prepared: biotin-conjugated PBQ (**B-PBQ**), aimed at capturing PBQ-binding proteins using magnetic beads, and fluorescence-modified PBQ (**J-PBQ**), aimed at confirming the distribution of PBQ in snails through *in situ* imaging. The successful preparation of **B-PBQ** (Figures S1–S3 Supporting Information online) and **J-PBQ** (Figures S4–S6) was confirmed by ^{1}H nuclear magnetic resonance (NMR), ^{13}C NMR, and high-resolution mass spectrometry (MS). Initially, the molluscicidal efficacy of different concentrations of **B-PBQ** (2, 4, and 6 mg/L) and **J-PBQ** (2.5, 5, and 10 mg/L) were tested at different time points (24, 48, and 72 h) (Table S1 Supporting Information online). With increasing time and compound concentration, the mortality rate of snails increased, reaching 41% for 6 mg/L **B-PBQ** and 86% for 10 mg/L **J-PBQ** within 72 h, suggesting that both probe molecules can effectively kill snails and exhibit time and concentration dependence. Despite a minor reduction in molluscicidal efficiency of the two modified probe molecules compared to PBQ, the modifications did not disrupt the active site (pyridine ring) responsible for molluscicidal activity and can be used for further testing to identify target

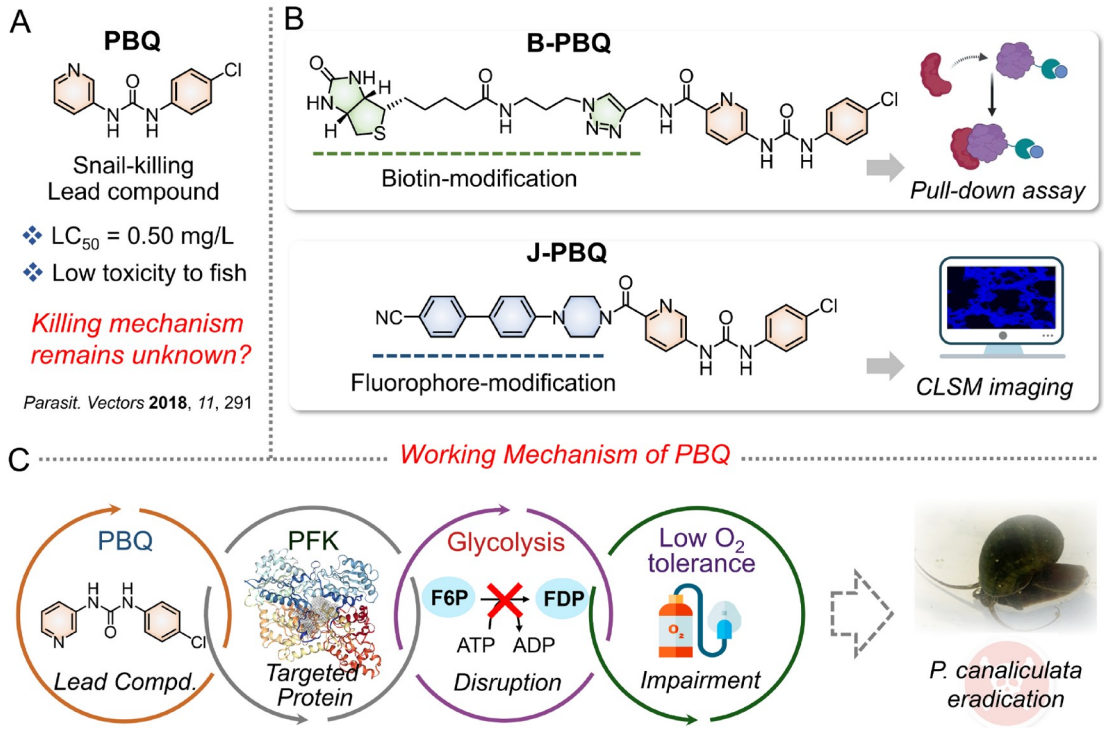

Scheme 1 (Color online) (A) Chemical structure of snail-killing lead compound PBQ. (B) Chemical structures of **B-PBQ** and **J-PBQ** were used for protein pull-down assays and CLSM imaging to determine the killing mechanism of PBQ. (C) The working mechanism of PBQ proposed in this work. PFK: phosphofructokinase; F6P: fructose-6-phosphate; FDP: fructose-1,6-bisphosphate.

proteins. Furthermore, after 72 h of exposure, the cytotoxicity of the two probes and PBQ on human normal liver (L02) cells for all three compounds was very low, with cell viability mostly above 90% (Figure S7). Specifically, only PBQ at a concentration of 40 μM exhibited relatively lower cell viability, approximately 60%, but this concentration is much higher than its effective molluscicidal concentration (1 mg/L ≈ 4 μM), indicating that PBQ and the two probes have low cytotoxicity on L02 cells, demonstrating good biosafety.

2.2 Chemical proteomic profiling and bioinformatics analysis reveal the candidate targets of PBQ

To capture the primary protein targets of PBQ in *P. canaliculata* snails, an integrated screening strategy combining chemical proteomic profiling and bioinformatics analysis was developed. First, **B-PBQ** was synthesized as a chemical probe for snail cellular lysate pull-down assay (Figure 1A). Soft tissue lysates of *P. canaliculata* snail were incubated with **B-PBQ**, followed by pulling-down with streptavidin-coated magnetic beads. A series of possible PBQ-interacting proteins were demonstrated by silver staining (Figure 1B) together with MS. The proteins specifically interacting with PBQ (n = 310) and the differentially expressed proteins [31] (DEPs, n = 218) that were significantly upregulated or downregulated in PBQ-treated *P. canaliculata* snails were overlapped, identifying an overlap of 19 proteins (Figure 1C and Table S2). Gene ontology enrichment analysis of the 19 proteins showed that the fructose-6-phosphate metabolic process was enriched (Figure 1D), in which PFK plays a key role. As PFK was also identified as a significantly down-regulated gene in a previous transcriptomic differential analysis [11], PFK was chosen as the study target.

2.3 PBQ engages PFK in a liver cellular context

To further verify that PFK is a target protein of PBQ, a newly designed cyanobiphenyl fluorophore was conjugated to PBQ with a formylpiperazine linker to generate the fluorescent probe **J-PBQ** (Figure 2A). The fluorescence properties of **J-PBQ** were analyzed through molecular calculations, fluorescence spectroscopy, quantum yield, and fluorescence lifetime experiments. The highest occupied molecular orbital (HOMO) and lowest unoccupied molecular orbital (LUMO) were calculated to be −5.23 and −1.45 eV (Figure 2B). Upon excitation at 336 nm, **J-PBQ** exhibited strong blue fluorescence at 466 nm with a quantum yield of 55.5% (Figure 2C and Figure S8) and a fluorescence lifetime of 1.076 ns (Figure S9), confirmed in solution. In ultraviolet (UV), **J-PBQ** retained the characteristic peaks of PBQ and exhibited new peaks (Figure 2D), confirming the success of the modification. Additionally, the fluorescence intensity of **J-PBQ** at 466 nm showed little variation, regardless of environmental pH or time lapse (Figure 2E). These results

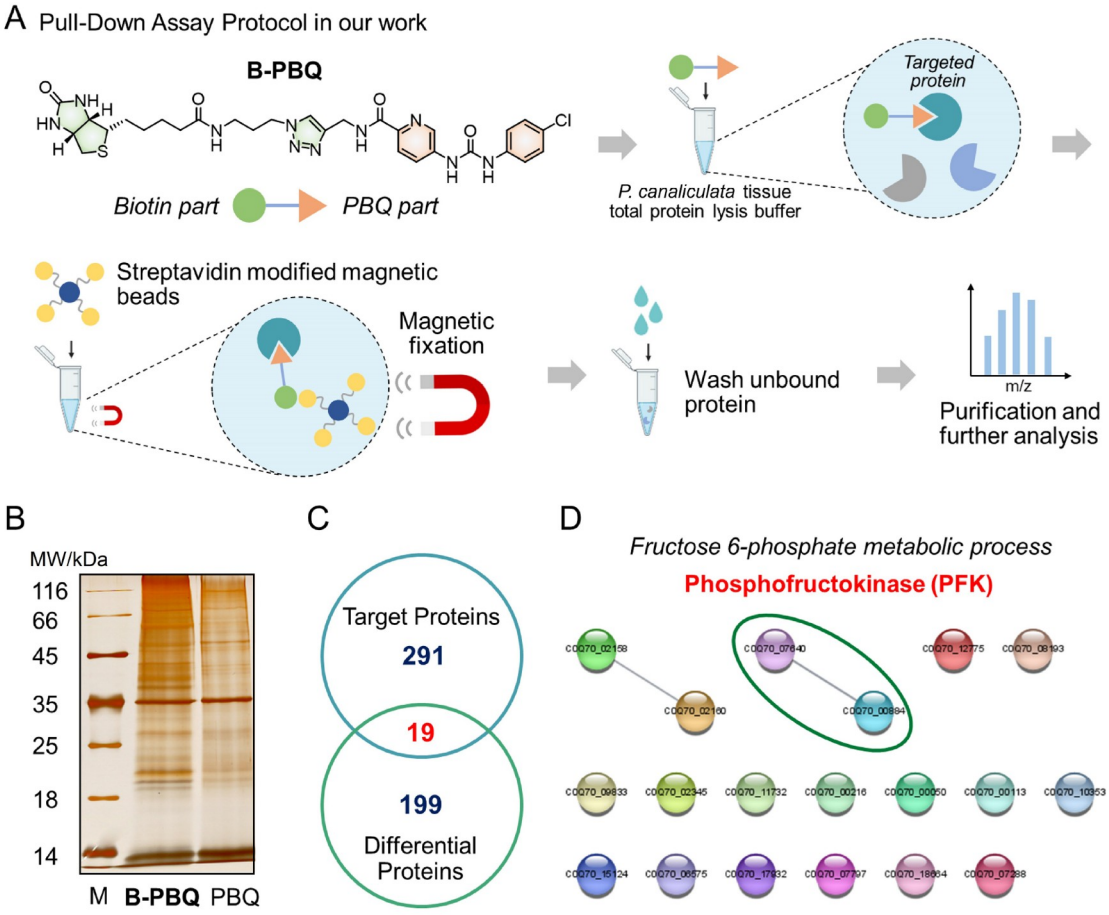

Figure 1 (Color online) (A) Protein pull-down assay protocol used in this work. (B) Silver staining results of pull-down proteins. (C) The overlap between the proteins specifically interacting with PBQ and the differentially expressed proteins. (D) Interaction network diagram of the 19 proteins reveals enrichment in the fructose-6-phosphate metabolic process.

demonstrate that the probe **J-PBQ** possesses excellent fluorescence performance. Thus, **J-PBQ** possesses excellent fluorescence performance. Given the effective molluscicidal efficacy and biological safety demonstrated by **J-PBQ** as described above, **J-PBQ** is suitable for *in vivo* distribution and fluorescence colocalization experiments. Drug distribution was visually examined using *ex vivo* fluorescence imaging of the major organs of *P. canaliculata*, showing that the molluscicide **J-PBQ** was mostly distributed and enriched in the liver compared to the intestine, foot, and stomach (Figures S10 and S11). Confocal laser scanning microscopy (CLSM) revealed that the **J-PBQ** (blue fluorescence) colocalized with PFK (green fluorescence) in the liver cellular context (Figure 2F), indicating that PFK is the target protein of **J-PBQ**. Additionally, based on molecular docking studies (Figure 2G and Figure S12), we propose that **J-PBQ** docks effectively into the natural hydrophobic pocket of PFK with a binding energy of −10.22 kcal/mol. This docking appears thermodynamically favored, which further supports the conclusion that PFK is the target protein of **J-PBQ**.

Thus, by using **B-PBQ** for protein pull-down assays and **J-PBQ** for CLSM imaging, we have, for the first time, identified and confirmed that PFK is the primary target protein of PBQ in *P. canaliculata*.

2.4 PBQ inhibits PFK catalytic activity and decreases PFK protein expression

Enzyme activity and content tests were conducted on liver tissue homogenate supernatant of *P. canaliculata* in different treatment groups using commercial assay kits. The PFK enzyme activities in the different treatment groups (Control -24 h, PBQ-0.5 mg/L-24 h, PBQ-1 mg/L-24 h, PBQ -2 mg/L-24 h, Control-72 h, and PBQ-1 mg/L-72 h) were 0.209 ± 0.023, 0.179 ± 0.035, 0.071 ± 0.023, 0.026 ± 0.032, 0.129 ± 0.023, and 0.019 ± 0.011 U/gprot, respectively (Figure 3A), whereas the PFK contents for the respective treatment groups were 6.066 ± 0.810, 5.158 ± 0.305, 3.228 ± 0.370, 2.047 ± 0.456, 4.629 ± 0.252, and 1.133 ± 0.091 ng/mL (Figure 3B). In the 24-h treatment group, both the enzyme activity and content of PFK decreased with increasing concentrations of PBQ. Under the

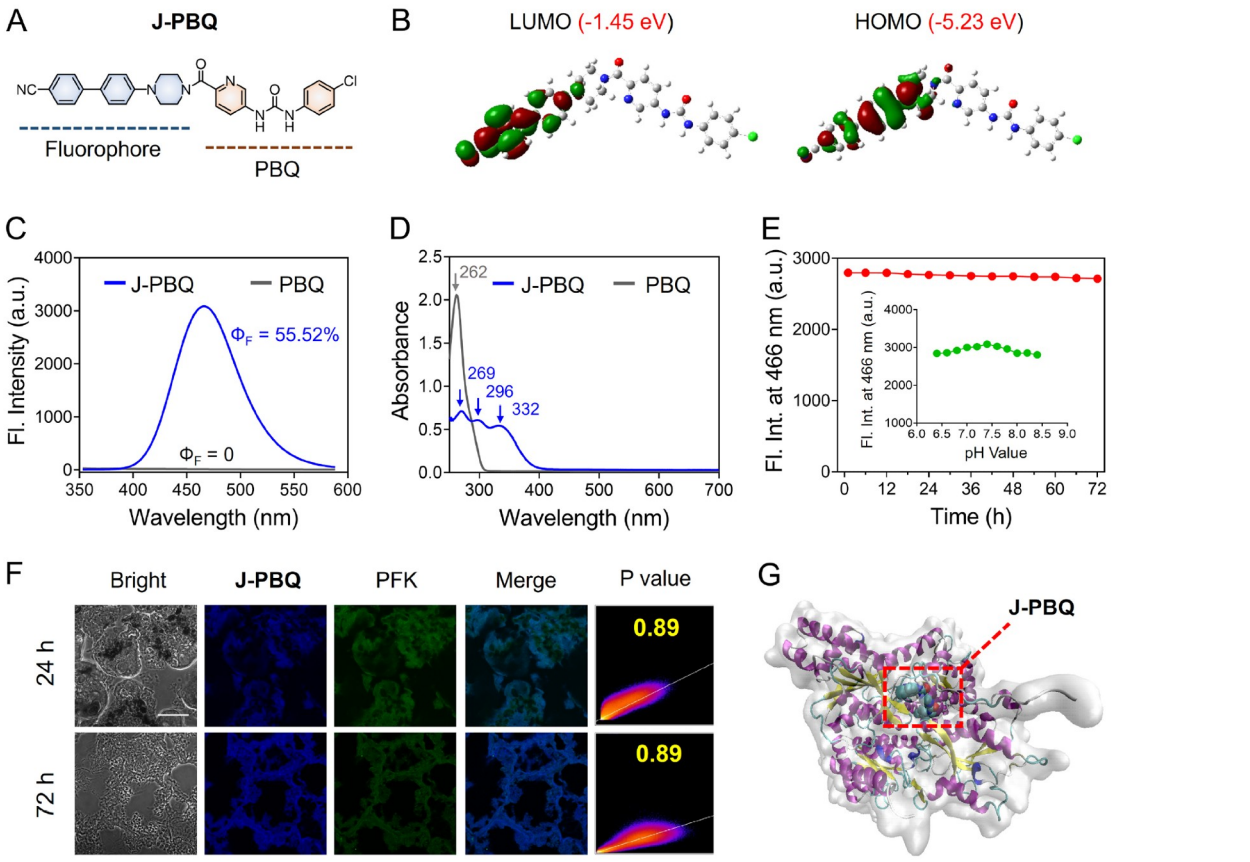

Figure 2 (Color online) (A) Design strategy of **J-PBQ**. (B) Frontier molecular orbitals and energies (eV) from density functional theory (DFT) calculations of **J-PBQ** in the ground state (S0). (C) Fluorescence spectroscopy of **J-PBQ** (10 μM) and PBQ (10 μM) in DMSO:PBS (v:v = 7:3, pH = 7.4), λ_{ex} = 336 nm. (D) UV absorption spectra of **J-PBQ** (10 μM) and PBQ (10 μM). (E) Fluorescence stability of **J-PBQ** over different time periods. Inset: fluorescence stability of **J-PBQ** in DMSO:PBS (v:v = 7:3) with different pH values (6.4–8.4). (F) Confocal imaging and colocalization analysis of snail liver sections after **J-PBQ** treatment in 24 and 72 h group. Scale bar: 20 μm. (G) Proposed molecular docking of **J-PBQ** into the pocket of PFK.

same concentration of PBQ (1 mg/L), the enzyme activity and content at 72 h were lower than those at 24 h, demonstrating that PBQ can inhibit the activity and content of PFK in the liver of *P. canaliculata*, and this inhibition is dependent on both concentration and time.

Subsequently, the effect of PBQ on the expression of PFK in the liver tissue of *P. canaliculata* was assessed through Western blot experiments and immunofluorescence assays. Protein extracts from the liver tissues of *P. canaliculata* from the different treatment groups were subjected to Western blot analysis to study the expression of PFK protein (Figure 3C). Changes in PFK expression in different treatment groups followed the same trend as those in PFK enzyme activity and content, consistent with the proteomic data. Thus, PBQ can inhibit the expression of PFK in the liver of *P. canaliculata*, and this inhibition is again dependent on concentration and time. Additionally, immunofluorescence experiments on frozen sections of *P. canaliculata* liver tissue also revealed similar findings (Figure 3D, Figures S13 and S14). Whether at 24 or 72 h after PBQ treatment, a decrease in the green fluorescence signal of the PFK channel was observed. Notably, the signal further diminished after 72 h compared to the 24 h. Thus, PBQ can inhibit the expression of PFK. Additionally, both **B-PBQ** and **J-PBQ** probes inhibited PFK content in the liver tissue of *P. canaliculata* after different durations of treatment (Figure S15), demonstrating that both compounds are effective.

In silico docking studies were conducted to identify the potential interaction mode between PBQ and PFK. PBQ was effectively docked into the natural hydrophobic pocket of PFK (Figure 3E) in a thermodynamically favorable process. The pyridine ring of PBQ was deeply embedded within the pocket formed by Met^{429}, Asn^{430}, Val^{431}, Met^{438}, Ile^{495}, and Cys^{497} residues, exhibiting a binding energy of −7.81 kcal/mol (Figure 3F). PBQ was primarily anchored through stable hydrogen bonding with the side chain of Val^{431} and other hydrophobic interactions. These results provide theoretical support for PBQ's potential to target and inhibit PFK in *P. canaliculata*.

PFK is the rate-limiting enzyme and a key branching point of glycolysis, which can catalyze the phosphorylation of F6P to FDP. To further confirm that PFK is the target of PBQ in *P. canaliculata*, FDP and F6P contents were measured in the liver tissue of *P. canaliculata* after PBQ treatment using

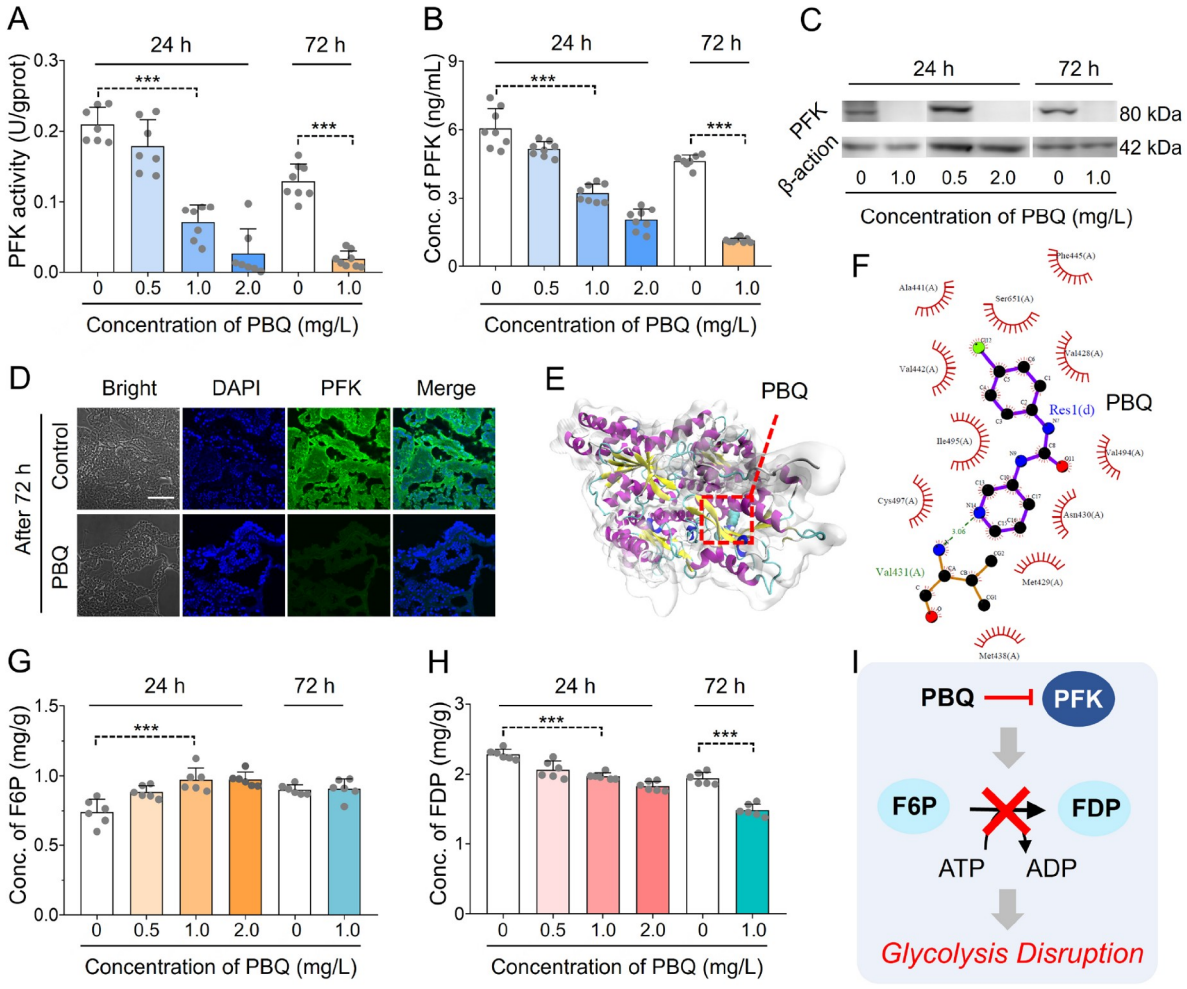

Figure 3 (Color online) (A) PFK enzyme activity results in the liver tissue of *P. canaliculata* in various groups with the treatment of different concentrations of PBQ. ***$P < 0.001$. (B) PFK content results in the liver tissue of *P. canaliculata* in various groups with the treatment of different concentrations of PBQ. ***$P < 0.001$. (C) Western blot results of protein expression in the liver tissue of *P. canaliculata* in various groups with the treatment of different concentration of PBQ. β-actin was used as an internal control. (D) Immunofluorescence results of frozen sections of the liver tissue of *P. canaliculata* in various groups with the treatment of different concentrations of PBQ. 4′,6-Diamidino-2-phenylindole (DAPI) channel: λ_{ex} = 359 nm; λ_{em} = 462 nm; PFK channel: λ_{ex} = 495 nm; λ_{em} = 519 nm. Scale bar: 50 μm. (E) Proposed molecular docking of PBQ into the pocket of PFK. (F) A schematic representation of the interactions between PBQ and PFK inferred from docking studies. (G) FDP content in the liver tissue of *P. canaliculata* in various groups with the treatment of different concentrations of PBQ. ***$P < 0.001$. (H) F6P content in the liver tissue of *P. canaliculata* in various groups with the treatment of different concentrations of PBQ. ***$P < 0.001$. (I) Targeted action of PBQ on PFK disrupts glycolysis in *P. canaliculata*, reducing energy supply and leading to its death.

commercial assay kits. The FDP contents in different treatment groups were 2.284 ± 0.067, 2.064 ± 0.011, 1.971 ± 0.043, 1.83 ± 0.062, 1.940 ± 0.078, and 1.489 ± 0.080 mg/g, respectively (Figure 3G). Thus, in the 24-h treatment group, FDP content gradually decreased with increasing PBQ concentration. The inhibition rate of the FDP content after 72 h of treatment with the same concentration of PBQ (1 mg/L) was 23.29% and lower than that after 24 h (13.71%), confirming that PBQ treatment reduces FDP content in the liver tissue of *P. canaliculata* in a concentration-dependent and time-dependent manner, consistent with the trend in PFK enzyme activity, content, and expression.

The F6P content in different treatment groups was 0.741 ± 0.084, 0.885 ± 0.041, 0.972 ± 0.078, 0.975 ± 0.047, 0.901 ± 0.032, and 0.908 ± 0.064 mg/g, respectively (Figure 3H). Thus, at 24 h, the F6P content tended to increase with increasing PBQ concentration, possibly due to the inhibition of PFK activity and expression by PBQ, leading to the inability of the substrate F6P to be converted into the product FDP. However, at 72 h, there was no significant difference in the F6P content between the PBQ treatment group and the control group, likely due to the involvement of other pathways in regulating F6P with increasing time.

The experimental results of FDP and F6P content suggested that PBQ inhibits the conversion of substrate F6P into product FDP in the liver tissue of *P. canaliculata*, likely due to the inhibition of PFK enzyme activity, content, and expression by PBQ, providing strong support for PFK being the

target protein of PBQ in *P. canaliculata*. Furthermore, the targeted action of PBQ on PFK leads to abnormal glycolysis in *P. canaliculata*, reducing energy supply, thereby causing the death of *P. canaliculata* (Figure 3I).

2.5 Differences in the effect of PBQ on PFK homologues explain the choice of target organisms

Following our previous studies showing that the lethal pesticidal ability of PBQ is restricted to mollusks and that it has a satisfactory safety profile for mammals and other non-target aquatic organisms, we hypothesized that the difference in the effect of PBQ on PFK homologues across species provides a potential explanation to this end. First, we analyzed the PFK homologues in multiple species from an evolutionary perspective. A phylogenetic tree was constructed based on the amino acid sequence homology of PFK covering *P. canaliculata*, a few other mollusks, and non-target species commonly seen in the snail habitat, and showed that in a phylogenetic position close to othernon-target species (Figure 4A). Second, in addition to *P. canaliculata*, PBQ also significantly decreased PFK levels in other two target snails *Oncomelania hupensis* and *Parafossarulus striatulus*; on the contrary, no significant change was observed in the non-target species *Danio rerio* (Figure 4B).

2.6 PBQ impairs the low-oxygen tolerance of *P. canaliculata*

Qiu's group [32] previously reported that *P. canaliculata* is more adapted to extreme environments, such as low oxygen, compared to native snails (*Pomacea diffusa*). Their studies found that the activity of PFK in *P. canaliculata* remained relatively unchanged in low-oxygen environments compared to normoxic conditions, which may contribute to its tolerance to low-oxygen environments [32]. Therefore, we hypothesized that PBQ could disrupt the low-oxygen tolerance of *P. canaliculata* by inhibiting its PFK activity and thereby affecting the glycolytic pathway, leading to the death of *P. canaliculata*. To test this hypothesis, we evaluated the survival rates of *P. canaliculata* under different oxygen concentrations (2, 4, and 6 mg/L) and PBQ concentrations (0, 0.5, 1, and 2 mg/L) at varying time points (24, 48, and 72 h). As the dissolved oxygen concentration in the water decreased, the concentration of PBQ increased, and the exposure time lengthened, the mortality rate of *P. canaliculata* also increased (Figure 5A–C). *P. canaliculata* can survive for 72 h under low-oxygen conditions (2 mg/L); however, PBQ significantly promotes the death of *P. canaliculata* in this environment. These results confirm that PBQ can disrupt the low-oxygen tolerance of *P. canaliculata*, possibly by targeting and inhibiting the PFK enzyme.

3 Conclusions

Through the modification of biotin and fluorophores on PBQ, we successfully prepared two small-molecule probes, **B-PBQ** and **J-PBQ**, to investigate the targeted killing mechanism of PBQ against *P. canaliculata*. Using **B-PBQ** in protein pull-down assays and **J-PBQ** in CLSM imaging, we identified and confirmed that PFK in *P. canaliculata* is the primary target of PBQ. Molecular docking studies further supported the interaction between PBQ and PFK. Subsequent experiments showed that PBQ inhibits the activity,

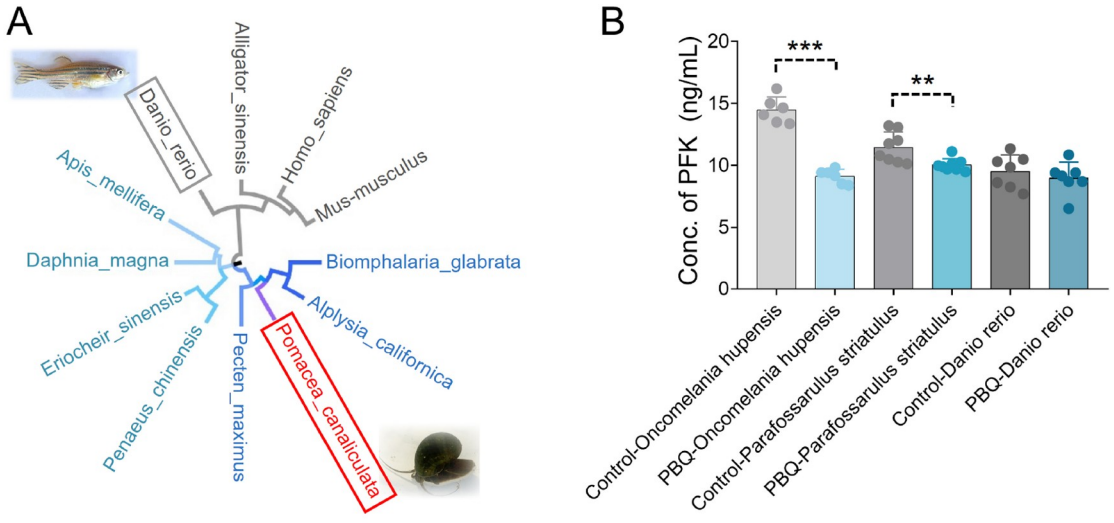

Figure 4 (Color online) (A) Phylogenetic tree of PFK proteins from different species (*Mus musculus*; *Homo sapiens*; *Alligator sinensis*; *Danio rerio*; *Apis mellifera*; *Daphnia magna*; *Eriocheir sinensis*; *Penaeus chinensis*; *Pecten maximus*; *Pomacea canaliculata*; *Aplysia californica*; *Biomphalaria glabrata*). (B) PFK content in the liver after 72 h of exposure to PBQ (1 mg/L) in different species (*Oncomelania hupensis*, *Parafossarulus striatulus*, *Danio rerio*). $^{**}P < 0.01$, $^{***}P < 0.001$.

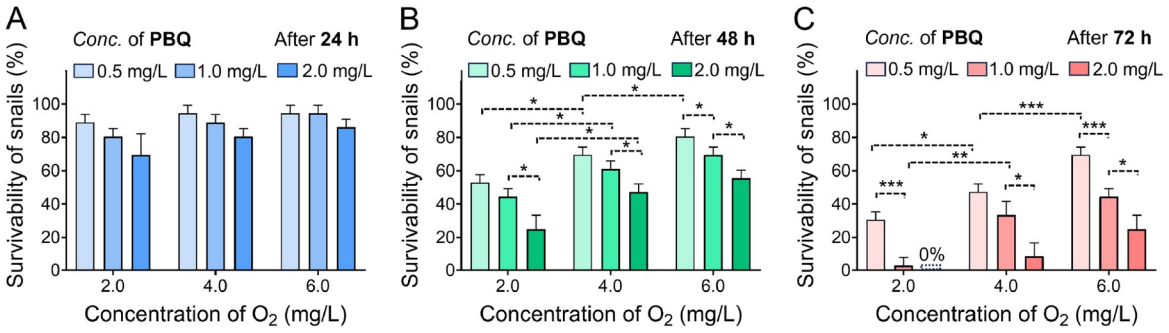

Figure 5 (Color online) Effect of different oxygen (O_2) concentrations and varying PBQ concentrations on the survival of snails after (A) 24 h, (B) 48 h, and (C) 72 h. *P < 0.05, **P < 0.01, ***P < 0.001.

content, and expression of PFK in the liver of *P. canaliculata*, with effects that are dependent on both concentration and time. Additionally, detection of FDP and F6P levels confirmed that PBQ affects both the products and substrates of PFK, reinforcing the conclusion that PFK is the target protein of PBQ. Testing PFK content across other species and constructing a phylogenetic tree of homologous proteins suggested that the selective killing of *P. canaliculata* by PBQ may be due to its specific inhibition of PFK. Moreover, efficacy tests under varying oxygen concentrations demonstrated that PBQ impairs the glycolysis pathway and decreases the low-oxygen tolerance of *P. canaliculata* by inhibiting PFK. These findings highlight the potential for developing PFK-targeted snail-killing pesticides. Additionally, the combined strategy of pull-down assays and optical imaging used in this study offers a novel approach for the exploration of mechanisms of other pesticide candidates.

Acknowledgements This work was supported by the National Natural Science Foundation of China (82072309, 22067019, 22367023, 32160236), the Major Science and Technology Project of Yunnan Province (202402AE090006), the Yunnan Provincial Science and Technology Department-Yunnan University Joint Special Project (202201BF070001-001), and the Three-Year Initiative Plan for Strengthening Public Health System Construction in Shanghai (2023–2025) Key Discipline Project (GWV1-11.1-12). Authors thank Advanced Analysis and Measurement Center of Yunnan University for the sample testing service. Authors also thank Professor Jianwen Qiu of Hong Kong Baptist University for his guidance and assistance.

Conflict of interest The authors declare no conflict of interest.

Supporting information The supporting information is available online at http://chem.scichina.com and http://link.springer.com/journal/11426. The supporting materials are published as submitted, without typesetting or editing. The responsibility for scientific accuracy and content remains entirely with the authors.

1 Seuffert ME, Martín PR. *Aquat Sci*, 2023, 86: 17
2 Liu C, Zhang Y, Ren Y, Wang H, Li S, Jiang F, Yin L, Qiao X, Zhang G, Qian W, Liu B, Fan W. *GigaScience*, 2018, 7: giy101
3 Giannelli A, Cantacessi C, Colella V, Dantas-Torres F, Otranto D. *Trends Parasitol*, 2016, 32: 255–264
4 Song L, Wang X, Yang Z, Lv Z, Wu Z. *Parasitol Res*, 2016, 115: 913–923
5 Martín PR, Burela S, Seuffert ME, Tamburi NE, Saveanu L. *CABI Rev*, 2019, 1–11
6 Sokolow SH, Wood CL, Jones IJ, Lafferty KD, Kuris AM, Hsieh MH, De Leo GA. *Trends Parasitol*, 2018, 34: 23–40
7 Kadri H, Lambourne OA, Mehellou Y. *ChemMedChem*, 2018, 13: 1088–1091
8 Andrews P, Thyssen J, Lorke D. *Pharmacol Ther*, 1982, 19: 245–295
9 Coelho P, Caldeira RL. *Infect Dis Poverty*, 2016, 5: 57
10 Gething KJ, Pickwell A, Chadd RP, Wood PJ. *Environ Pollut*, 2020, 265: 115015
11 Wang W, Huang S, Liu F, Sun Y, Wang X, Yao J, Li S, Liu Y, Luo B, Zhang X, Hu H, Deng Z, Duan L. *J Agric Food Chem*, 2022, 70: 1079–1089
12 Chen Z, Wang W, Yao J, Li S, Zhang X, Hu H, Liu X, Luo B, Liu Y, Xu H, Duan L. *Chemosphere*, 2019, 222: 56–61
13 Wang W, Mao Q, Yao J, Yang W, Zhang Q, Lu W, Deng Z, Duan L. *Parasites Vectors*, 2018, 11: 291
14 Shi Q, Duan L, Qin Z, Wang W, Shen L, Hua X, Shen L', Cao J, Zhu F, Wu J, Li S. *TropicalMed*, 2022, 7: 294
15 Deng L, Huang X, Ren J. *Anal Chem*, 2020, 92: 7020–7027
16 Chang Y, Zhu D, Guo H, Yin X, Ding K, Li Z. *ChemBioChem*, 2019, 20: 1783–1788
17 Wang J, Zhang CJ, Chia WN, Loh CCY, Li Z, Lee YM, He Y, Yuan LX, Lim TK, Liu M, Liew CX, Lee YQ, Zhang J, Lu N, Lim CT, Hua ZC, Liu B, Shen HM, Tan KSW, Lin Q. *Nat Commun*, 2015, 6: 10111
18 Gao P, Liu YQ, Xiao W, Xia F, Chen JY, Gu LW, Yang F, Zheng LH, Zhang JZ, Zhang Q, Li ZJ, Meng YQ, Zhu YP, Tang H, Shi QL, Guo QY, Zhang Y, Xu CC, Dai LY, Wang JG. *Military Med Res*, 2022, 9: 30
19 Yu C, Wu D, Dai L, He X, Hou JT, Shen J, Li Z. *Coord Chem Rev*, 2023, 489: 215203
20 Li K, Xu S, Wang B, Huan S, Song X, Yuan L, Zhang XB. *Sci China Chem*, 2023, 66: 2425–2434
21 Fang H, Li P, Shen C, Tang F, Ding A, Bai H, Peng B, Yang X, Li Z, Huang K, Pan S, Li L, Huang W. *Sci China Chem*, 2023, 66: 2053–2061
22 Li D, Shen T, Xue X, Chen W, Tao W, Chi W, Liu SH, Tan Y, Liu X, Yin J. *Sci China Chem*, 2023, 66: 2329–2338
23 Wuo MG, Dulberger CL, Warner TC, Brown RA, Sturm A, Ultee E, Bloom-Ackermann Z, Choi C, Zhu J, Garner EC, Briegel A, Hung DT, Rubin EJ, Kiessling LL. *J Am Chem Soc*, 2024, 146: 17669–17678
24 Healey RD, Saied EM, Cong X, Karsai G, Gabellier L, Saint-Paul J, Del Nero E, Jeannot S, Drapeau M, Fontanel S, Maurel D, Basu S, Leyrat C, Golebiowski J, Bossis G, Bechara C, Hornemann T, Arenz C, Granier S. *Angew Chem Int Ed*, 2022, 61: e202109967
25 Kitamura K, Itoh H, Sakurai K, Dan S, Inoue M. *J Am Chem Soc*, 2018, 140: 12189–12199
26 Bayat M, Mardani H, Roghani-Mamaqani H, Hoogenboom R. *Chem*

Soc Rev, 2024, 53: 4045–4085
27 Lovell S, Zhang L, Kryza T, Neodo A, Bock N, De Vita E, Williams ED, Engelsberger E, Xu C, Bakker AT, Maneiro M, Tanaka RJ, Bevan CL, Clements JA, Tate EW. *J Am Chem Soc*, 2021, 143: 8911–8924
28 Chen L, Lyu Y, Zhang X, Zheng L, Li Q, Ding D, Chen F, Liu Y, Li W, Zhang Y, Huang Q, Wang Z, Xie T, Zhang Q, Sima Y, Li K, Xu S, Ren T, Xiong M, Wu Y, Song J, Yuan L, Yang H, Zhang XB, Tan W. *Sci China Chem*, 2023, 66: 1336–1383
29 Lu Y, Liao H, Li T, Sun W, Liang J, Zhao YQ, Zhao H, Zhou Y. *Sens Actuat B-Chem*, 2023, 377: 133030
30 Liu C, Yang S, Qiao Y, Zhao Y, Wang W, Jia M, He Y, Zhou Y, Duan L. *Chin Chem Lett*, 2021, 32: 1809–1813
31 Xu Y, Wang W, Yao J, Yang M, Guo Y, Deng Z, Mao Q, Li S, Duan L. *Mol Biochem Parasitol*, 2022, 247: 111431
32 Mu H, Sun J, Cheung SG, Fang L, Zhou H, Luan T, Zhang H, Wong CKC, Qiu JW. *J Proteomics*, 2018, 172: 36–48